21 NAND gate

21.1 General information

The problem is a system of 14 stiff IDEs of index 1. It has been contributed by Michael Günther and Peter Rentrop [GR96].

The software part of the problem is in the file nand.f available at [MM08].

21.2 Mathematical description of the problem

The problem is of the form:

$$C(y(t))\,\frac{\mathrm{d}y}{\mathrm{d}t} \;=\; f(t,y(t)), \qquad y(0)=y_0, \quad y'(0)=y_0' \tag{II.21.1}$$

with

$$y\in \mathbb{R}^{14}, \qquad 0\le t\le 80.$$

The equations are given by:

$$C_{GS}\cdot(\dot y_5-\dot y_1) = i_{DS}^D(y_2-y_1,y_5-y_1,y_3-y_5,y_5-y_2,y_4-V_{DD}) + \frac{y_1-y_5}{R_{GS}} \tag{II.21.2}$$

$$C_{GD}\cdot(\dot y_5-\dot y_2) = -i_{DS}^D(y_2-y_1,y_5-y_1,y_3-y_5,y_5-y_2,y_4-V_{DD}) + \frac{y_2-V_{DD}}{R_{GD}}, \tag{II.21.3}$$

$$C_{BS}(y_3-y_5)\cdot(\dot y_5-\dot y_3) = \frac{y_3-V_{BB}}{R_{BS}} - i_{BS}^D(y_3-y_5), \tag{II.21.4}$$

$$C_{BD}(y_4-V_{DD})\cdot(-\dot y_4) = \frac{y_4-V_{BB}}{R_{BD}} - i_{BD}^D(y_4-V_{DD}), \tag{II.21.5}$$

$$\begin{aligned} &C_{GS}\cdot\dot y_1 + C_{GD}\cdot\dot y_2 + C_{BS}(y_3-y_5)\cdot\dot y_3 - (C_{GS}+C_{GD}+C_{BS}(y_3-y_5)+C_5)\cdot\dot y_5 \\ &-C_{BD}(y_9-y_5)\cdot(\dot y_5-\dot y_9) \;=\; \tfrac{y_5-y_1}{R_{GS}} + i_{BS}^D(y_3-y_5) + \tfrac{y_5-y_7}{R_{GD}} + i_{BD}^E(y_9-y_5), \end{aligned} \tag{II.21.6}$$

$$C_{GS}\cdot\dot y_6 = -i_{DS}^E(y_7-y_6,V_1(t)-y_6,y_8-y_{10},V_1(t)-y_7,y_9-y_5) + C_{GS}\cdot\dot V_1(t) - \frac{y_6-y_{10}}{R_{GS}}, \tag{II.21.7}$$

$$C_{GD}\cdot\dot y_7 = i_{DS}^E(y_7-y_6,V_1(t)-y_6,y_8-y_{10},V_1(t)-y_7,y_9-y_5) + C_{GD}\cdot\dot V_1(t) - \frac{y_7-y_5}{R_{GD}}, \tag{II.21.8}$$

$$C_{BS}(y_8-y_{10})\cdot(\dot y_8-\dot y_{10}) = -\frac{y_8-V_{BB}}{R_{BS}} + i_{BS}^E(y_8-y_{10}), \tag{II.21.9}$$

$$C_{BD}(y_9-y_5)\cdot(\dot y_9-\dot y_5) = -\frac{y_9-V_{BB}}{R_{BD}} + i_{BD}^E(y_9-y_5), \tag{II.21.10}$$

$$\begin{aligned} &C_{BS}(y_8-y_{10})\cdot(\dot y_8-\dot y_{10}) - C_{BD}(y_{14}-y_{10})\cdot(\dot y_{10}-\dot y_{14}) + C_{10}\cdot\dot y_{10} \\ &= \tfrac{y_{10}-y_6}{R_{GS}} + i_{BS}^E(y_8-y_{10}) + \tfrac{y_{10}-y_{12}}{R_{GD}} + i_{BD}^E(y_{14}-y_{10}), \end{aligned} \tag{II.21.11}$$

$$C_{GS}\cdot\dot y_{11} = -i_{DS}^E(y_{12}-y_{11},V_2(t)-y_{11},y_{13},V_2(t)-y_{12},y_{14}-y_{10}) + C_{GS}\cdot\dot V_2(t) - \frac{y_{11}}{R_{GS}}, \tag{II.21.12}$$

$$C_{GD}\cdot\dot y_{12}=i^E_{DS}(y_{12}-y_{11},V_2(t)-y_{11},y_{13},V_2(t)-y_{12},y_{14}-y_{10})+C_{GD}\cdot\dot V_2(t)-\frac{y_{12}-y_{10}}{R_{GD}},\quad \text{(II.21.13)}$$

$$C_{BS}(y_{13})\cdot\dot y_{13}=-\frac{y_{13}-V_{BB}}{R_{BS}}+i^E_{BS}(y_{13}),\quad \text{(II.21.14)}$$

$$C_{BD}(y_{14}-y_{10})\cdot(\dot y_{14}-\dot y_{10})=-\frac{y_{14}-V_{BB}}{R_{BS}}+i^E_{BD}(y_{14}-y_{10}).\quad \text{(II.21.15)}$$

The functions C_{BD} and C_{BS} read

$$C_{BD}(U)=C_{BS}(U)=\begin{cases} C_0\cdot\left(1-\frac{U}{\phi_B}\right)^{-\frac12} & \text{for}\quad U\le 0,\\ C_0\cdot\left(1+\frac{U}{2\cdot\phi_B}\right) & \text{for}\quad U>0\end{cases}$$

with $C_0=0.24\cdot10^{-4}$ and $\phi_B=0.87$.

The functions i^D_{BS} and i^E_{BS} have the same form denoted by i_{BS}. The only difference between them is that the constants used in i_{BS} depend on the superscript D and E. The same holds for the functions $i^{D/E}_{BD}$ and $i^{D/E}_{DS}$. The functions i_{BS}, i_{BD} and i_{DS} are defined by

$$\begin{aligned} i_{BS}(U_{BS}) &= \begin{cases} -i_S\cdot\left(\exp(\frac{U_{BS}}{U_T})-1\right) & \text{for}\quad U_{BS}\le 0,\\ 0 & \text{for}\quad U_{BS}>0,\end{cases}\\ i_{BD}(U_{BD}) &= \begin{cases} -i_S\cdot\left(\exp(\frac{U_{BD}}{U_T})-1\right) & \text{for}\quad U_{BD}\le 0,\\ 0 & \text{for}\quad U_{BD}>0,\end{cases}\end{aligned}$$

$$i_{DS}(U_{DS},U_{GS},U_{BS},U_{GD},U_{BD})=\begin{cases} GDS_+(U_{DS},U_{GS},U_{BS}) & \text{for}\quad U_{DS}>0,\\ 0 & \text{for}\quad U_{DS}=0,\\ GDS_-(U_{DS},U_{GD},U_{BD}) & \text{for}\quad U_{DS}<0,\end{cases}$$

where

$$GDS_+(U_{DS},U_{GS},U_{BS})=$$

$$\begin{cases} 0 & \text{for}\quad U_{GS}-U_{TE}\le 0,\\ -\beta\cdot(1+\delta\cdot U_{DS})\cdot(U_{GS}-U_{TE})^2 & \text{for}\quad 0<U_{GS}-U_{TE}\le U_{DS},\\ -\beta\cdot U_{DS}\cdot(1+\delta\cdot U_{DS})\cdot(2\cdot(U_{GS}-U_{TE})-U_{DS}) & \text{for}\quad 0<U_{DS}<U_{GS}-U_{TE},\end{cases}$$

with

$$U_{TE}=U_{T0}+\gamma\cdot\left(\sqrt{\Phi-U_{BS}}-\sqrt{\Phi}\right),\quad \text{(II.21.16)}$$

and

$$GDS_-(U_{DS},U_{GD},U_{BD})=$$

$$\begin{cases} 0 & \text{for}\quad U_{GD}-U_{TE}\le 0,\\ \beta\cdot(1-\delta\cdot U_{DS})\cdot(U_{GD}-U_{TE})^2 & \text{for}\quad 0<U_{GD}-U_{TE}\le -U_{DS},\\ -\beta\cdot U_{DS}\cdot(1-\delta\cdot U_{DS})\cdot(2\cdot(U_{GD}-U_{TE})+U_{DS}) & \text{for}\quad 0<-U_{DS}<U_{GD}-U_{TE},\end{cases}$$

with

$$U_{TE}=U_{T0}+\gamma\cdot\left(\sqrt{\Phi-U_{BD}}-\sqrt{\Phi}\right).\quad \text{(II.21.17)}$$

The constants used in the definition of i_{BS}, i_{BD} and i_{DS} carry a superscript D or E. Using for example the constants with superscript E in the functions i_{BS} yields the function i^E_{BS}. These constants are shown in Table II.21.1. The other constants are given by

TABLE II.21.1: *Dependence of constants on D and E for i_{BS}, i_{BD} and i_{DS}.*

	E	D
i_S	10^{-14}	10^{-14}
U_T	25.85	25.85
U_{T0}	0.2	-2.43

	E	D
β	$1.748 \cdot 10^{-3}$	$5.35 \cdot 10^{-4}$
γ	0.035	0.2
δ	0.02	0.02
Φ	1.01	1.28

$$\begin{aligned} V_{BB} &= -2.5, \\ V_{DD} &= 5, \\ C_5 &= C_{10} = 0.5 \cdot 10^{-4}, \\ R_{GS} &= R_{GD} = 4, \\ R_{BS} &= R_{BD} = 10, \\ C_{GS} &= C_{GD} = 0.6 \cdot 10^{-4}. \end{aligned}$$

The functions $V_1(t)$ and $V_2(t)$ are

$$V_1(t) = \begin{cases} 20 - tm & \text{if} \quad 15 < tm \leq 20, \\ 5 & \text{if} \quad 10 < tm \leq 15, \\ tm - 5 & \text{if} \quad 5 < tm \leq 10, \\ 0 & \text{if} \quad tm \leq 5, \end{cases}$$

with $tm = t \bmod 20$ and

$$V_2(t) = \begin{cases} 40 - tm & \text{if} \quad 35 < tm \leq 40, \\ 5 & \text{if} \quad 20 < tm \leq 35, \\ tm - 15 & \text{if} \quad 15 < tm \leq 20, \\ 0 & \text{if} \quad tm \leq 15, \end{cases}$$

with $tm = t \bmod 40$. From these definitions for $V_1(t)$ and $V_2(t)$ we see that the function f in (II.21.1) has discontinuities in its derivative at $tm = 5, 10, 15, 20$. Therefore, we restart the solvers at $t = 5, 10, \ldots, 75$.

Consistent initial values are given by $y_0' = 0$ and

$$\begin{aligned} &y_1 = y_2 = y_5 = y_7 = 5.0, \\ &y_3 = y_4 = y_8 = y_9 = y_{13} = y_{14} = V_{BB} = -2.5, \\ &y_6 = y_{10} = y_{12} = 3.62385, \\ &y_{11} = 0. \end{aligned}$$

All components of y are of index 1.

It is clear from Formulas (II.21.16) and (II.21.17) that the function f can not be evaluated if one of the values $\Phi - U_{BS}$, $\Phi - U_{BD}$ or Φ becomes negative. To prevent this situation, we set `IERR=-1` in the Fortran subroutine that defines f if this happens. See page *IV-ix* of the the description of the software part of the test set for more details on `IERR`.

21.3 Origin of the problem

The NAND gate in Figure II.21.1 consists of two n-channel enhancement MOSFETs (ME), one n-channel depletion MOSFET (MD) and two load capacitances C_5 and C_{10}. MOSFETs are special transistors, which have four terminals: the drain, the bulk, the source and the gate, see also Figure II.21.3. The drain voltage of MD is constant at $V_{DD} = 5$[V]. The bulk voltages are constantly $V_{BB} = -2.5$[V]. The gate voltages of both enhancement transistors are controlled by two voltage

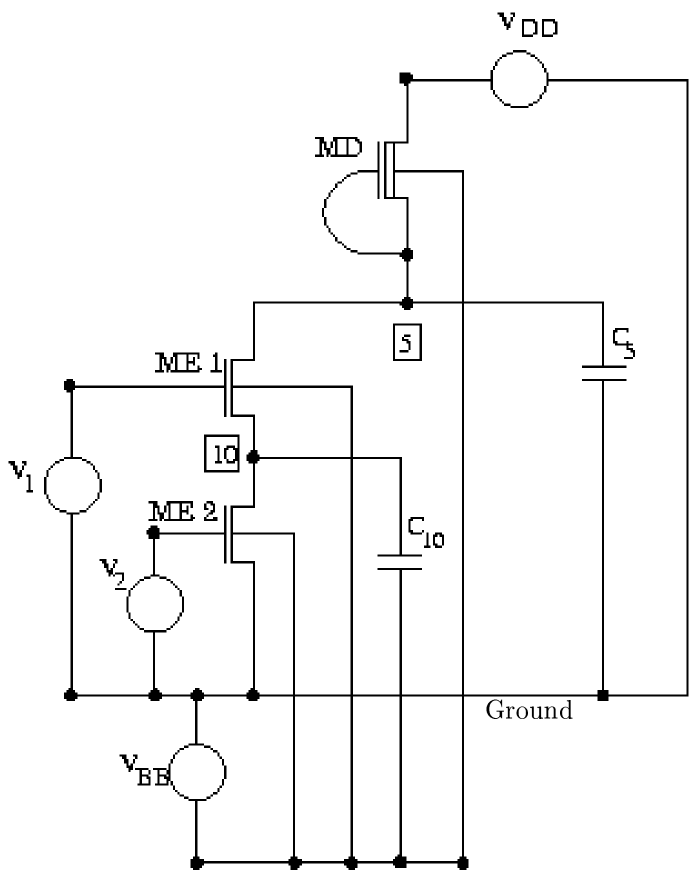

FIGURE II.21.1: *Circuit diagram of the NAND gate (taken from [GR96])*

sources V_1 and V_2. Depending on the input voltages, the NAND gate generates a response at node 5 as shown in Figure II.21.2. If we represent the logical values 1 and 0 by high respectively low voltage levels, we see that the NAND gate executes the *N*ot *AND* operation. This behavior can be explained from Figure II.21.1 as follows. Roughly speaking, a transistor acts as a switch between drain and source; it closes if the voltage between gate and source drops below a certain threshold value. The circuit is constructed such that the voltage at node 10 drops to zero unless V_1 is high and V_2 is low, in which case it is approximately 5[V]. This means that as soon either V_1 or V_2 is low, then the corresponding enhancement transistors lock; the voltage at node 5 is high at $V_{DD} = 5$[V] due to MD. If both V_1 and V_2 exceed a given threshold voltage, then a drain current through both enhancement transistors occurs. The MOSFETs open and the voltage at node 5 breaks down. The response is low. In the circuit analysis the three MOSFETs are replaced by the circuit shown in Figure II.21.3. Here, the well-known companion model of Shichmann and Hodges [SH68] is used. The characteristics of the circuit elements can differ depending on the MD or ME case. This circuit has four internal nodes indicated by 1, 2, 3 and 4. The static behavior of the transistor is described by the drain current i_{DS}. To include secondary effects, load capacitances like R_{GS}, R_{GD}, R_{BS}, and R_{BD} are introduced. The so-called *pn*-junction between source and bulk is modeled by the diode i_{BS} and the non-linear capacitance C_{BS}. Analogously, i_{BD} and C_{BD} model the *pn*-junction between bulk and drain. Linear gate capacitances C_{GS} and C_{GD} are used to describe the intrinsic charge flow effects roughly.

		V2	
		LOW	HIGH
V1	LOW	HIGH	HIGH
	HIGH	HIGH	LOW

FIGURE II.21.2: *Response of the NAND gate*

To formulate the circuit equations, we note that the circuit consists of 14 nodes. These 14 nodes are the nodes 5 and 10 and the 12 internal nodes of the three transistors. For every node a variable is introduced that represents the voltage in that node. Table II.21.2 shows the variable–node correspondence. In terms of these voltages the circuit equations are formulated by using the Kirchoff Current Law (KCL) along with the transistor model shown in Figure II.21.3. In Figure II.21.4, we check the

TABLE II.21.2: *Correspondence between variables and nodes*

variables	nodes
1–4	internal nodes MD-transistor
5	node 5
6–9	internal nodes ME1-transistor
10	node 10
11–14	internal nodes ME2-transistor

behavior of the NAND gate by plotting V_1 and V_2 together with the numerical value for the voltage at node 5, which is obtained as y_{10} in §21.4. The picture confirms that the NAND gate produces a high signal in the intervals $[0, 5]$, $[10, 15]$, $[20, 25]$, $[40, 45]$, $[50, 55]$ and $[60, 65]$, whereas the output signal on $[30, 35]$ and $[70, 75]$ is low.

We remark that in this description the unit of time is the nanosecond, while in the report [GR96] the unit of time is the second.

21.4 Numerical solution of the problem

Tables II.21.3–II.21.4 and Figures II.21.5–II.21.7 present the reference solution at the end of the integration interval, the run characteristics, the behavior of the solution over the integration interval and the work-precision diagram, respectively. In computing the scd values, only y_5, the response of the gate at node 5, was considered. The reference solution was computed on the Cray C90, using PSIDE with Cray double precision and atol = rtol = 10^{-16}. For the work-precision diagram, we used: rtol = $10^{-(4+m/8)}$, $m = 0, 1, \ldots, 64$; atol = rtol, h0 = rtol for MEBDFI. .

.

References

[GR96] M. Günther and P. Rentrop. The NAND-gate – a benchmark for the numerical simulation of digital circuits. In W. Mathis and P. Noll, editors, *2.ITG-Diskussionssitzung "Neue Anwendungen Theoretischer Konzepte in der Elektrotechnik" - mit Gedenksitzung zum 50. Todestag von Wilhelm Cauer*, pages 27–33, Berlin, 1996. VDE-Verlag.

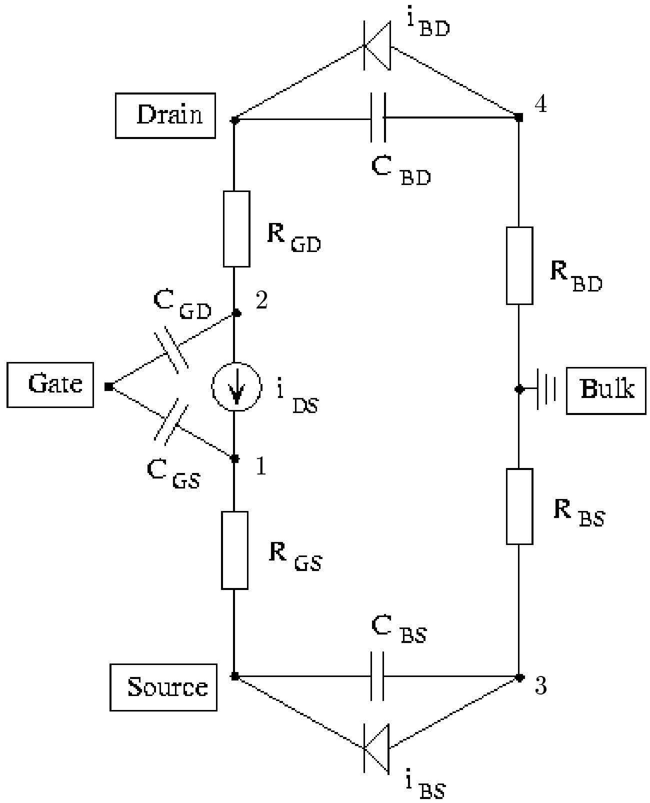

FIGURE II.21.3: *Companion model of a MOSFET (taken from [GR96])*

[MM08] F. Mazzia and C. Magherini. *Test Set for Initial Value Problem Solvers, release 2.4*. Department of Mathematics, University of Bari and INdAM, Research Unit of Bari, February 2008. Available at http://www.dm.uniba.it/~testset.

[SH68] H. Shichman and D.A. Hodges. Insulated-gate field-effect transistor switching circuits. *IEEE J. Solid State Circuits*, SC-3:285–289, 1968.

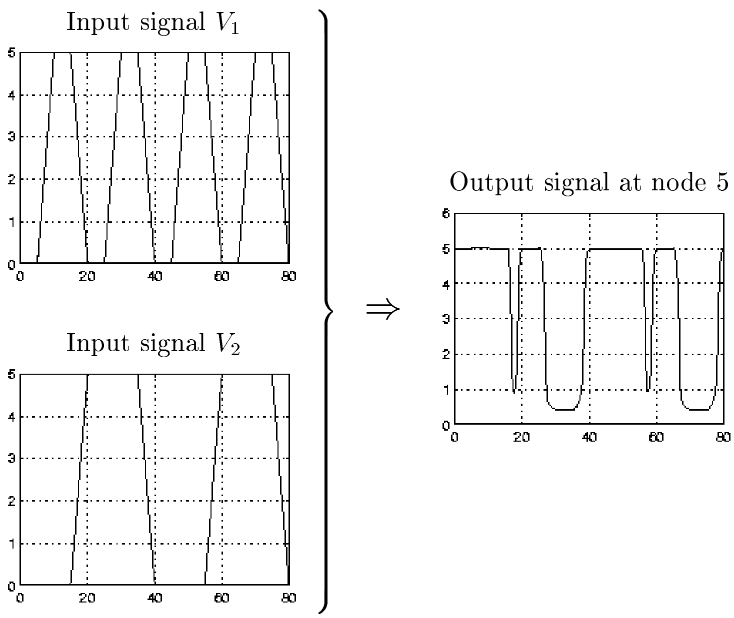

FIGURE II.21.4: *Plots of V_1, V_2 and the output of the NAND gate.*

TABLE II.21.3: *Reference solution at the end of the integration interval.*

y_1	$0.4971088699385777 \cdot 10$	y_8	$-0.2500077409198803 \cdot 10$
y_2	$0.4999752103929311 \cdot 10$	y_9	$-0.2499998781491227 \cdot 10$
y_3	$-0.2499998781491227 \cdot 10$	y_{10}	-0.2090289583878100
y_4	$-0.2499999999999975 \cdot 10$	y_{11}	$-0.2399999999966269 \cdot 10^{-3}$
y_5	$0.4970837023296724 \cdot 10$	y_{12}	-0.2091214032073855
y_6	-0.2091214032073855	y_{13}	$-0.2499999999999991 \cdot 10$
y_7	$0.4970593243278363 \cdot 10$	y_{14}	$-0.2500077409198803 \cdot 10$

TABLE II.21.4: *Run characteristics.*

solver	rtol	atol	h0	mescd	scd	steps	accept	#f	#Jac	#LU	CPU
DDASSL	10^{-4}	10^{-4}		3.69	5.25	1037	951	1639	246		0.0459
	10^{-7}	10^{-7}		6.22	8.81	3825	3604	5207	638		0.1376
MEBDFI	10^{-4}	10^{-4}	10^{-4}	3.76	4.57	1120	1006	7693	249	249	0.0683
	10^{-7}	10^{-7}	10^{-7}	6.24	7.50	3786	3429	24487	755	755	0.2255
PSIDE-1	10^{-4}	10^{-4}		2.39	3.33	464	411	6574	109	1796	0.0927
	10^{-7}	10^{-7}		5.28	8.48	773	643	13134	222	2760	0.1796

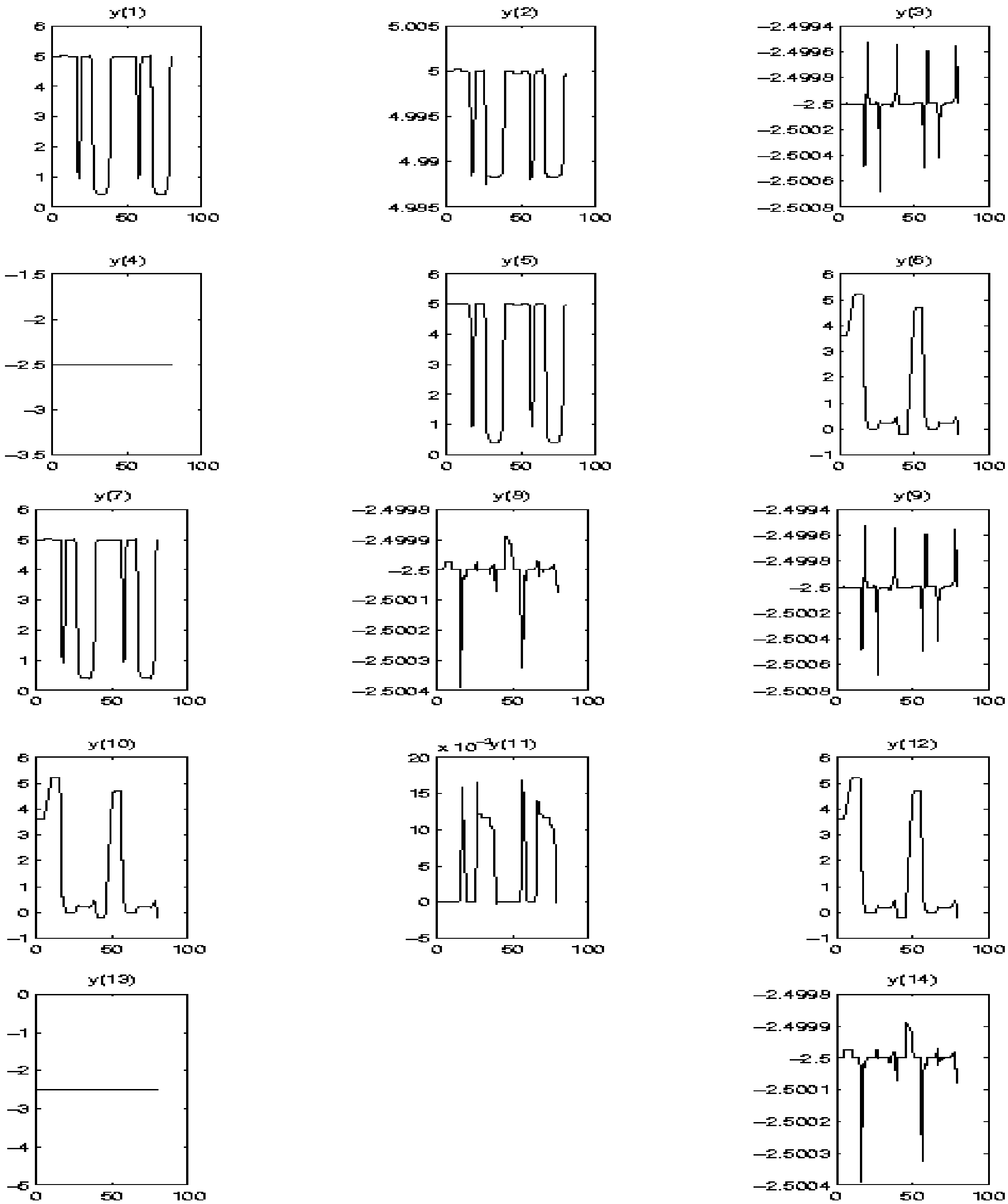

FIGURE II.21.5: *Behavior of the solution over the integration interval.*

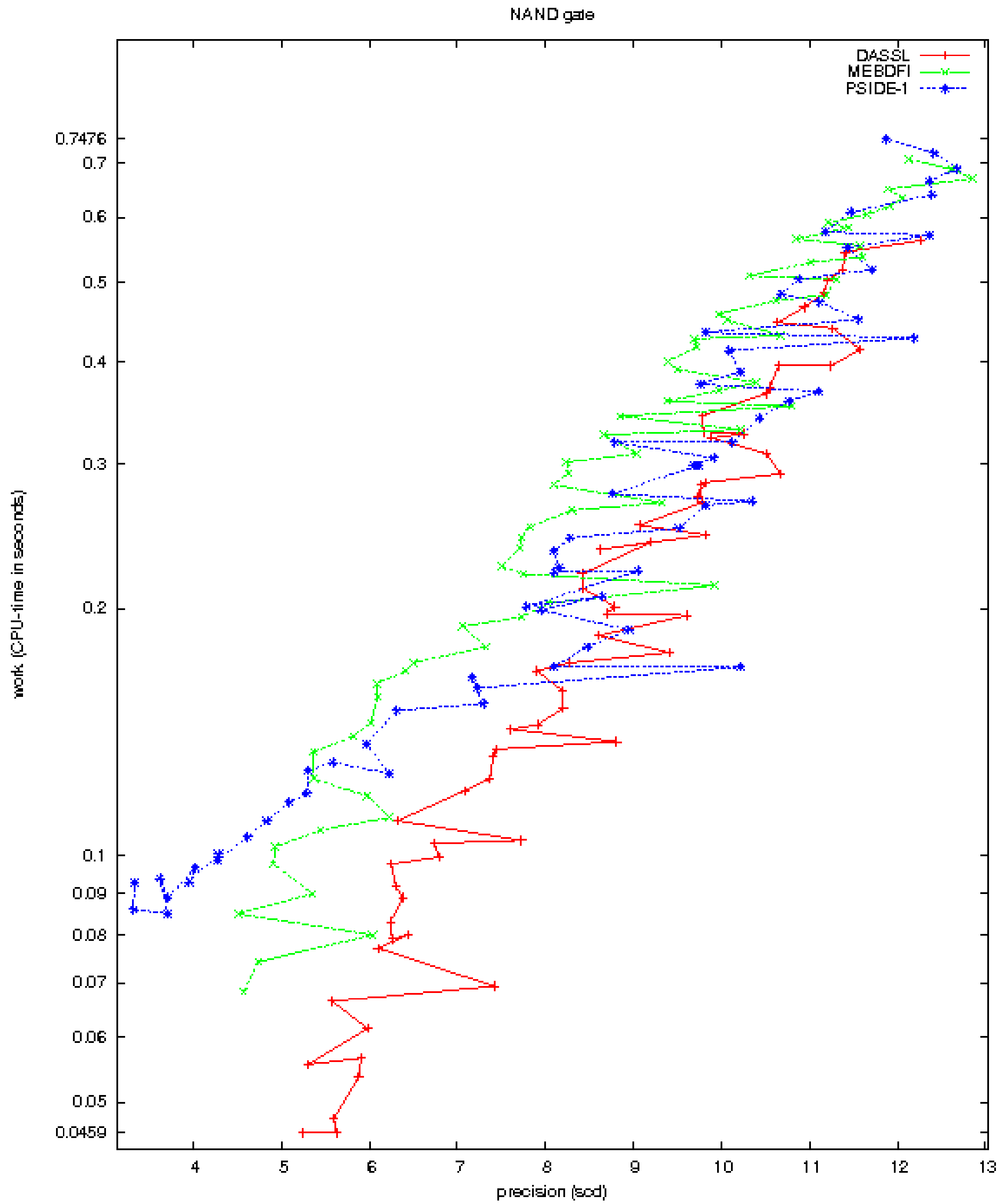

FIGURE II.21.6: *Work-precision diagram (scd versus CPU-time).*

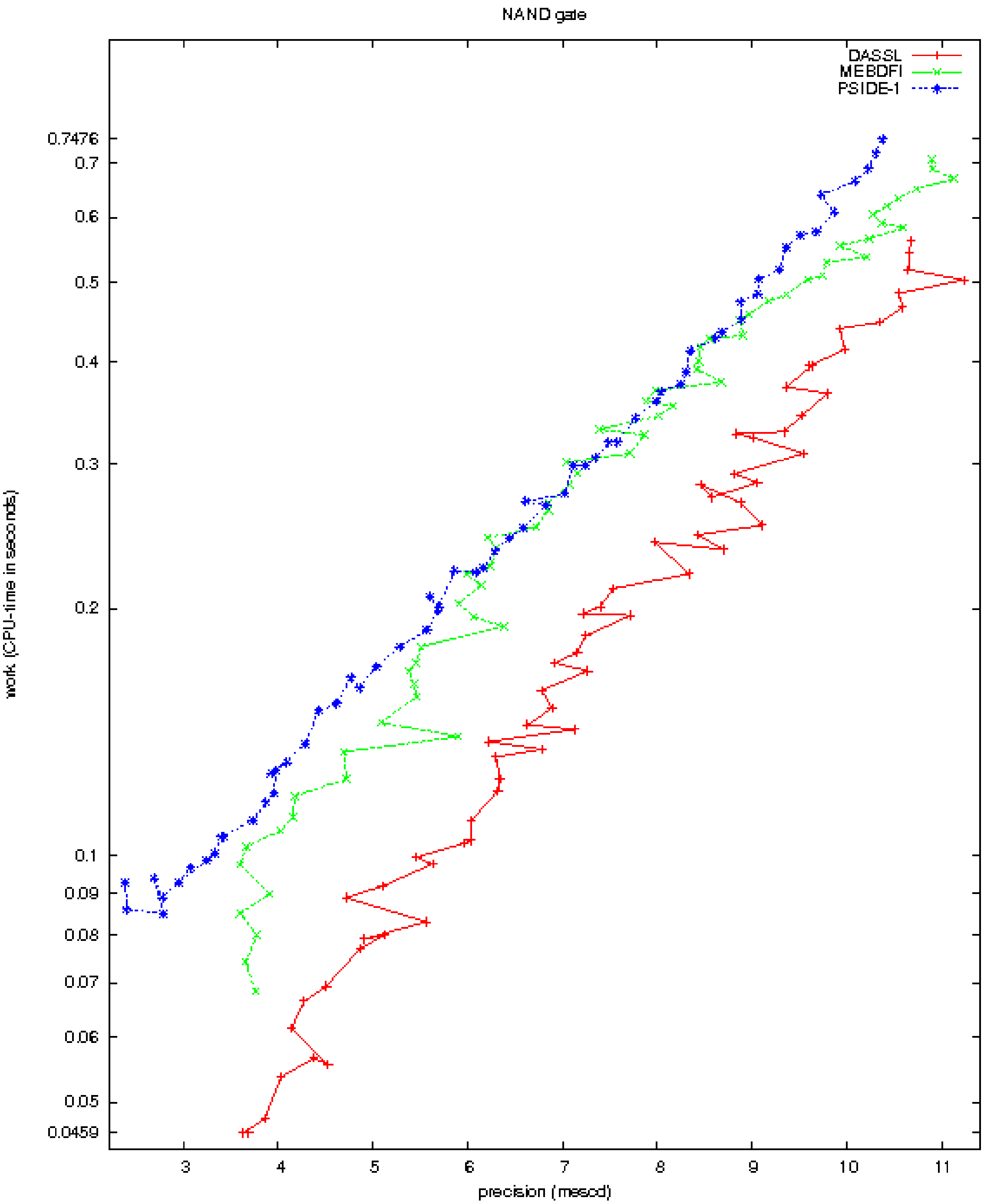

FIGURE II.21.7: *Work-precision diagram (mescd versus CPU-time).*